

## **Puffing and Microexplosion Behaviour of Parent-Child Droplets of Water in Pure Diesel Emulsion during Leidenfrost Effect**

Mohammed Yahaya Khan <sup>\*1</sup>, Z.A.Abdul Karim<sup>1</sup>, A. Rashid A. Aziz<sup>1</sup>, M R Heikal<sup>2</sup>, C. Crua<sup>2</sup>

<sup>1</sup>Centre for Automotive Research and Electric Mobility (CAREM),

Department of Mechanical Engineering, Universiti Teknologi PETRONAS, Malaysia

<sup>2</sup>Sir Harry Ricardo Laboratories, School of Computing, Engineering and Mathematics,  
University of Brighton, United Kingdom

\*Corresponding author: mohammedyahayakhan@yahoo.com

### **Abstract**

The microexplosion evolution phenomenon of single droplets of water in pure diesel emulsion under Leidenfrost effect has been studied. The tested emulsions were stabilized with a blend of commercial surfactants with three different water contents of 9%, 12% and 15%. A high speed camera synchronized with backlight technique was used to capture the evolution of microexplosion and puffing. Three different droplet diameters of approximately 2.6mm, 2mm and 0.2mm were analysed. It was found that the tendency of microexplosion and puffing frequency was influenced by the droplet diameter. It was also observed that the child droplets ejected from the parent droplet undergoes further puffing processes. The waiting time for microexplosion and puffing were compared for different droplets size.

### **Introduction**

In spite of their preferable advantages, diesel engines are one of the foremost pollution contributors to the environment. One way to combat these drawbacks of compression ignition (CI) engines can be overcome by fuel based solutions, which can be readily adapted to the existing engines without any modifications. Emulsified fuels are considered as one of the conceivable alternative fuels for reducing the engine exhaust emissions. The most noticeable effects of such fuels are the secondary atomization occurring during the combustion process. The volatility difference between the base fuel and the dispersed water droplets (i.e) results in superheating of the water which is achieved before the base fuel and rapid vapour expansion which leads to a violent microexplosion of the emulsified droplets [1]. The presence of water aids to reduce the combustion temperature, therefore reducing NO<sub>x</sub>. The microexplosion phenomena results in the formation of smaller droplets with very high surface-to-volume ratio which results in better mixing with air leading to more complete combustion and lower particulate matter (PM) emissions.

The microexplosion phenomenon is often quoted for countering the engine exhaust emissions (i.e.) reducing PM and NO<sub>x</sub> simultaneously. Therefore, understanding the microexplosion phenomena can help to increase the efficiency of alternative fuels, in particular with water in diesel emulsions. Usage of suspended droplets on thermocouple or quartz fiber has been studied previously to record the temperature history of the heated emulsion droplets, (i.e) emulsion of pyrolysis oil in diesel oil [2], n-dodecane and n-tetradecane in water emulsion [3], kerosene and water emulsion [4], commercial diesel and water emulsion [5], and diesel- bio diesel-ethanol blends [6]. One of the main demerits in these type of techniques is that the presence of thermocouple or the fiber wire results in the heterogeneous bubble nucleation on the surface of the wire [1].

Also, prior studies confirmed that the microexplosion does not always occur [5, 7, 8]. The droplet diameters considered for the purpose of visualization of the microexplosion evolution were different among the studies. Emulsion fuels with the parent droplet size, studied previously by the other researchers for the development of microexplosion phenomenon are highlighted in the Table 1. This experimental work investigates the evolution of microexplosion phenomenon of water in pure diesel emulsion droplets. Breakup characterisation studies of child droplets are scarce and are limited to base fuels other than pure diesel [6]. Such characteristics are also studied here by analyzing the primary and secondary droplet sizes in order to fill in this gap in the knowledge base. The droplets sizes studied in this experiment are within the comparable range of other researchers, so as to compare the present results with their works.

**Table 1.** Droplet sizes and emulsion fuels on previous studies

Reference	Emulsion fuels used	Parent droplet diameter (mm)
Rafael et al. [9]	Heavy fuel oil/water	0.83
Tanaka et al. [10]	n-dodecane + n-tetradecane + n-hexadecane + water	2
Watanabe et al. [4]	kerosene/water	0.7-1.3
Morozumi et al. [11]	n-hexadecane/water	1.5-1.8
Suzuki et al. [12]	kerosene/water	0.85-0.99
Dominique et al. [13]	sunflower oil/water	0.15-0.45
Califano et al. [5]	commercial diesel/water	0.7-1.1
Mura et al. [14]	sunflower oil/water	1

## Materials and methods

### Emulsion preparation and stability

The Water in Diesel Emulsions (WiDE) used in this study was blended at 1500rpm for 15 minutes using overhead stirrer. Mixtures of commercial surfactants Span-80 with an HLB value of 4.3 and an HLB of 11 for TWEEN 85 were used as emulsifier. Surfactants are necessary to lower the interfacial tension between the diesel and water to form a stable emulsion. The base fuel used was pure diesel without any additives. The emulsions were stabilized with 15% of surfactant concentration to the water content. The preparation matrix for the WiDE is shown in Table 2. All the prepared emulsions were found to be stable for almost 30 days. This was due to the dosage of surfactant blend being sufficient to the overall surface of the dispersed compound to be completely covered by the surfactant molecules [15].

A Hydrophilic-Lipophilic Balance (HLB) value of 9 was used for stabilizing all the emulsions. It was obtained by mixing the two surfactants by the following equation

$$\% A = 100 * (x - HLB_B) / (HLB_A - HLB_B) \quad (1)$$

Where

$HLB_A$  = HLB value of surfactant A

$HLB_B$  = HLB value of surfactant B

$x$  = Required HLB value

% A = Quantity of surfactant A required

% B = Quantity of surfactant B required

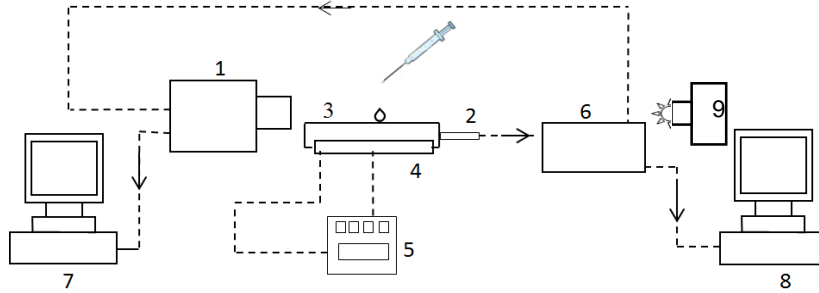
**Table 2.** The preparation matrix for the WiDE

Volume of surfactant	Sample ID	Amount of H <sub>2</sub> O (ml)	Volume (ml)	
			Diesel	Surfactant
15% from H <sub>2</sub> O	WiDE-1	9	89.65	1.35
	WiDE-2	12	86.20	1.8
	WiDE-3	15	82.75	2.25

### Experimental Setup

Schematic diagram of the experimental setup for the evolution of microexplosion visualization is shown in Figure 1. A PHANTOM MIRO M310 high speed camera was used for image capturing. The image acquisition rate was set at 8000 fps for larger droplets and 10000 fps with a resolution of 640X480 for droplets with the smallest diameter. A polished flat aluminum plate with a small concave dint was used to place the droplet and the base plate temperature was maintained at 500 +/- 2°C using a ceramic heater to obtain the Leidenfrost effect. The temperature was maintained throughout the experiment by a digital temperature controller. The water droplets distribution images were captured by using a digital microscope with a magnification of 1000X and the Sauter mean diameter of dispersed water droplets were calculated by post processing the images obtained. The light source used for backlight illumination purpose was of single LED type and was synchronized with the exposure time of the high speed camera. Also, a light source with 12 high power LEDs was used for direct image recording to observe the phase changes and internal features of the droplet during the evolution of microexplosion. The

recording speed was set at 2000 fps with a resolution of 510X510 pixels. The images were post processed using the phantom camera control software for measurements and calculating the waiting time of microexplosion. Approximately 2.6 mm and 2 mm sized droplets diameters of water in pure diesel emulsion (WiDE) were generated using a syringe of 0.8mm and 0.4mm orifice diameter needles. The smallest WiDE droplet with a diameter of 0.2 mm (approximate) was generated by dropping larger droplets from a height onto the hot aluminium plate. The high speed camera was set to start recording the events as soon as the droplet touched the hot plate with a pre-trigger option. This facilitated the identification of the exact starting time during post processing of the captured images.



1. High Speed Camera 2. Thermocouple for hot plate 3. Hot plate 4. Ceramic heater 5. Temperature controller for hot plate 6. N.I. Controller 7&8. PC for Data Acquisition and Image processing. 9. Light source for backlight illumination

**Figure 1.** Microexplosion visualization schematic diagram

## Results and discussion

The water droplet distribution in the emulsions was captured using a digital microscope with a magnification of 1000X as shown in Figure 2. The water droplet diameter measurements were made using the Motic Image plus 2.0 software.

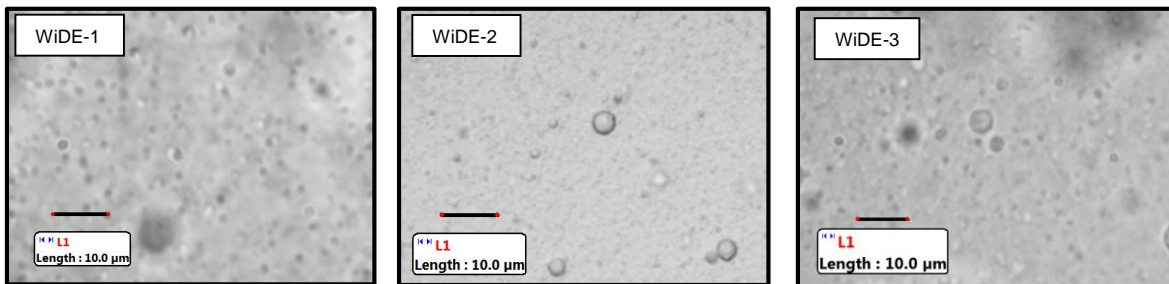
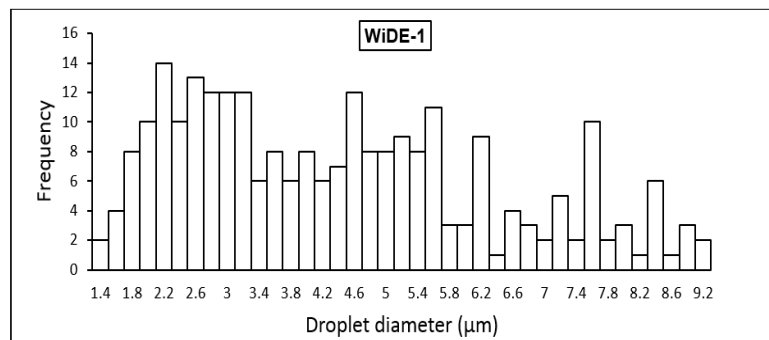


**Figure 2.** Images of WiDE, from left to right, with 9%, 12% and 15% water content

The sizes of the measured droplets were expressed in terms of Sauter Mean Diameter (SMD) ( $D_{32}$ ) as follow:

$$D_{32} = \frac{\sum_i (n_i \times D_i^3)}{\sum_i (n_i \times D_i^2)} \quad (2)$$

Where  $D_i$  is the diameter of the droplet and  $n_i$  is the total number of droplets having the same diameter. The size distribution of water droplets of the samples are depicted in Figure 3.



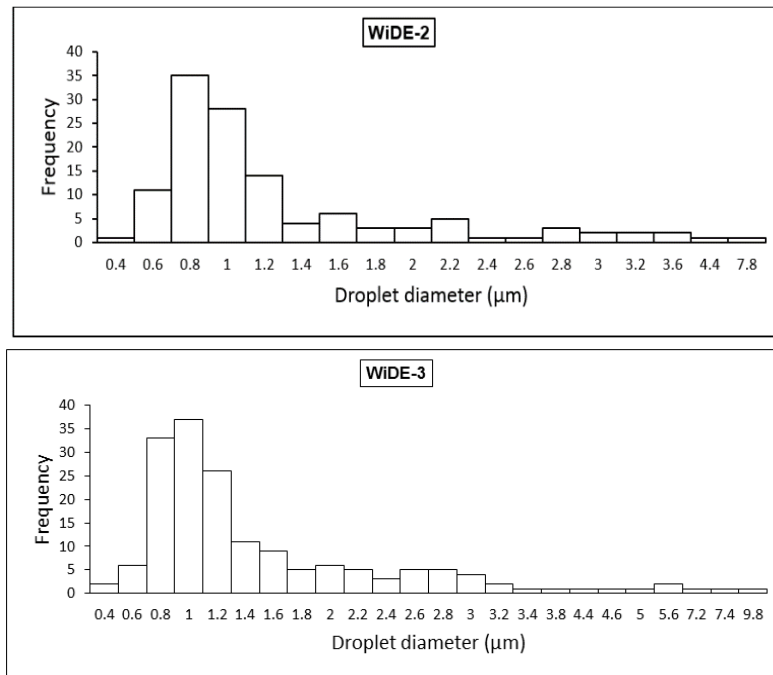


**Figure 3.** The size distribution of water droplets of WiDE samples

It is clear from Figure 3 that WiDE-1 had a wide range of distributed water droplet diameters even with sizes of 7.6 to 8.4  $\mu\text{m}$ . Whereas, WiDE-2 had 0.8 to 1.2  $\mu\text{m}$  and WiDE-3 had 0.8 to 1.4  $\mu\text{m}$  diameter droplets which were more densely populated.

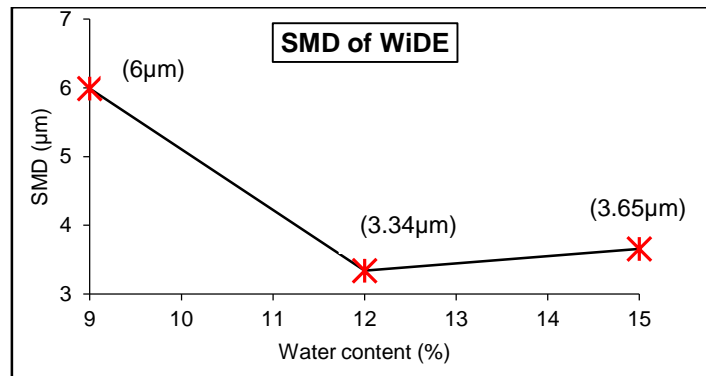


**Figure 4.** Sauter mean diameter (SMD) of WiDE vs water content

For the same surfactant dosage, the SMD of WiDE-1 was around 6  $\mu\text{m}$ , 3.34  $\mu\text{m}$  for WiDE-2 and 3.65  $\mu\text{m}$  WiDE-3 as shown in Figure 4. In the case of WiDE-1, the surfactant dosage for 9% water content might be in excess and resulted in the formation of larger and uneven size distribution of water droplets whereas, the difference between the droplet diameters for WiDE-2 and WiDE-3 were very small. Many researchers reported that the higher the surfactant concentrations then the longer is the emulsion stability and vice versa. Contradictory, Wasan et al.[16] reported that over dosage of surfactant destabilize the emulsion because of rapid coalescence.

**Table 3.**Physical properties of WiDE

Sample ID	Density @ 20°C (g/m <sup>3</sup> )	Viscosity @ 40°C (m pas)	Surface tension @ 20°C (mN/m)
Pure diesel	0.84376	2.7396	-----
WiDE-1	0.86109	3.4223	27.47
WiDE-2	0.86052	3.6863	32.27
WiDE-3	0.87140	4.6791	31.11

Physical properties of the prepared emulsions are tabulated in the Table 3. The density of the emulsions was found to be almost the same for all the WiDE samples and the viscosity was increasing with increasing water content. The surface tension of WiDE-1 was lower compared to the other two samples.

#### Microexplosion evolution of WiDE with bigger parent droplet

The evolution of WiDE  $\phi 2.6$  mm (approx.) size droplets is shown in Figure 5. Since no significant changes in the emulsion phase were observed in the early part of the experiment after the placing of the droplet on the surface, the image sequence shown is from 2 seconds onwards and was captured using the direct image recording.

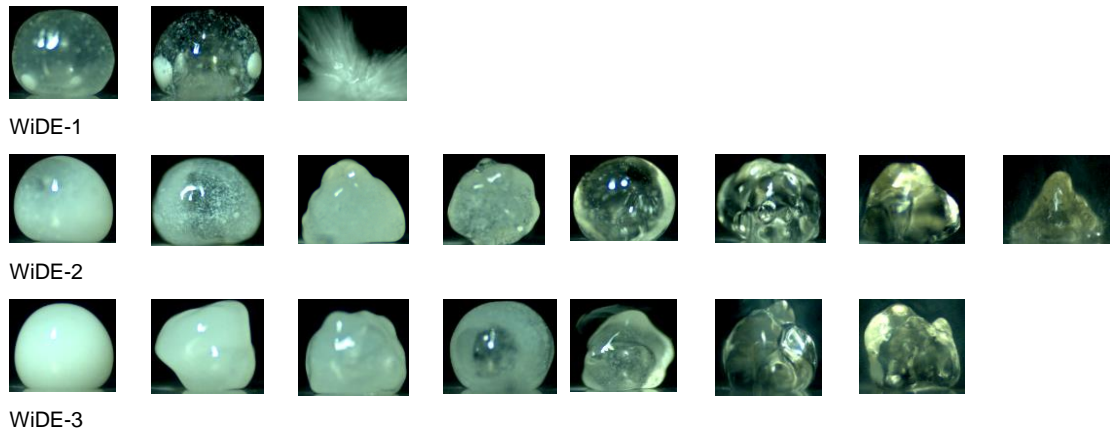


**Figure 5.** Evolution of  $\phi 2.6$ mm droplets WiDE-1, 2 and 3 at every 0.5s time interval

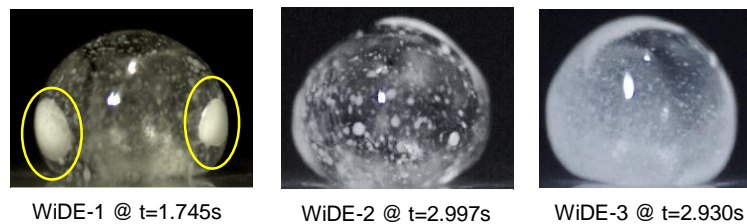


**Figure 6.** Images showing the phase change of emulsions with 9%, 12%, and 15% water content with time interval

The rate of coalescence to form larger dispersed water droplets was found to be more dominant (as highlighted in Figure 6) in the emulsion WiDE-1 with 9% water, hence more readily exploded when compared to the other two WiDE samples. The phase change for all the WiDE with  $\phi 2.6$ mm is shown in Figure 6 for selected times. It is clear from these images that the coalescence is more dominant in case of WiDE-1 than the other two emulsions. Also, the coalescence leading to phase change occurred earlier than the other WiDE emulsions. As shown in Figure 3, WiDE-1 contains a wide range of different sized dispersed water droplets compared to the other two WiDE samples. This non uniform distribution of water droplets and also the excessive surfactant dosage with respect to the water content led to a higher coalescence rate and hence resulted in microexplosion. Whereas, the other two WiDE samples had narrow sized distributed water droplets, with a minimum difference in the values of the SMD, did not undergo coalescence resulting in only phase change with no microexplosion.

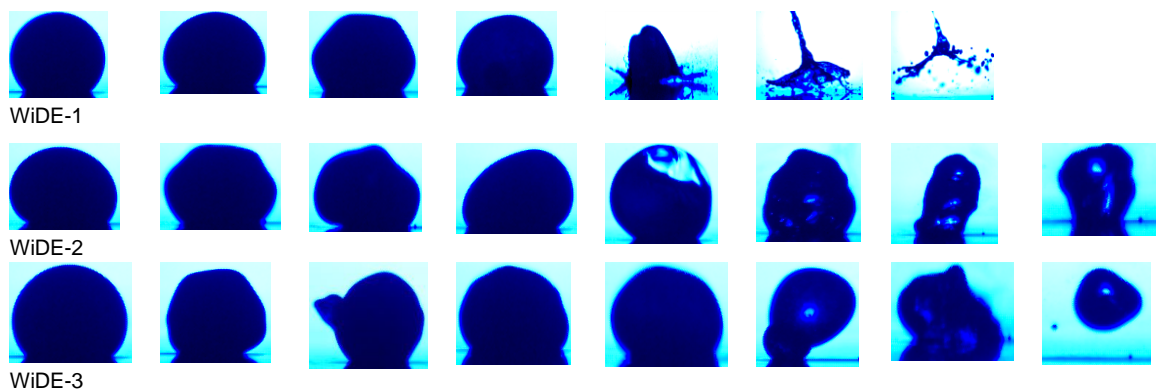


**Figure 7.** Evolution of  $\phi 2.0$ mm droplets WiDE-1, 2 and 3 at every 0.5s time interval

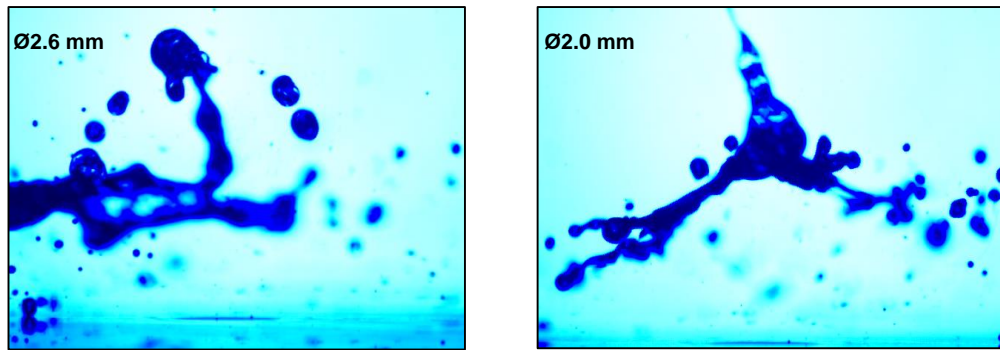


**Figure 8.** Secondary droplets after microexplosion of  $\phi 2.6$  mm and  $\phi 2.0$  mm WiDE-1 parent droplets

The sequence of evolution of the  $\phi 2.0$  mm is shown in Figure 7. The images shown are from 0 second and with a time interval of 0.5 seconds. Similar behaviour occurred in the case of droplets with  $\phi 2.0$  mm (approx.) in which WiDE-1 developed microexplosion whereas the other two emulsions did not. The secondary droplets after microexplosion from WiDE-1 are shown in Figure 8. Further observation of the secondary droplets from a  $\phi 2.6$  mm parent droplet were in the average size of  $\phi 0.22$  mm with a standard deviation of 0.181 and the secondary droplets from the  $\phi 2.0$  mm parent droplet were around  $\phi 0.19$  mm with a standard deviation of 0.112. From these observations it can be concluded that the size of the secondary droplets is influenced by the size of the parent droplet itself.

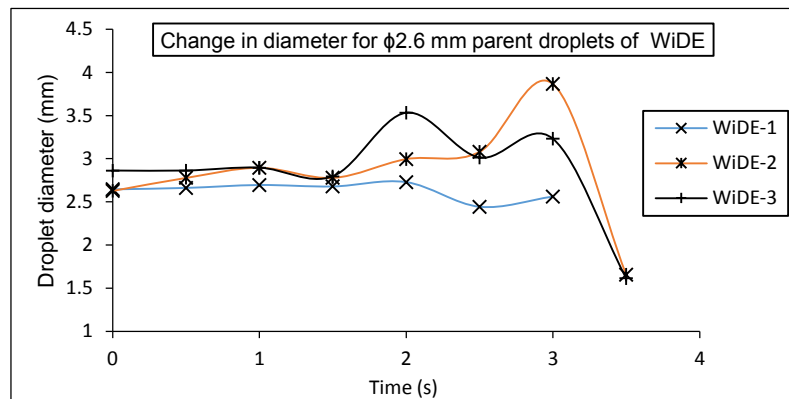


**Figure 9.** Change in diameter of  $\phi 2.6$  mm WiDE droplets at every 0.5s interval

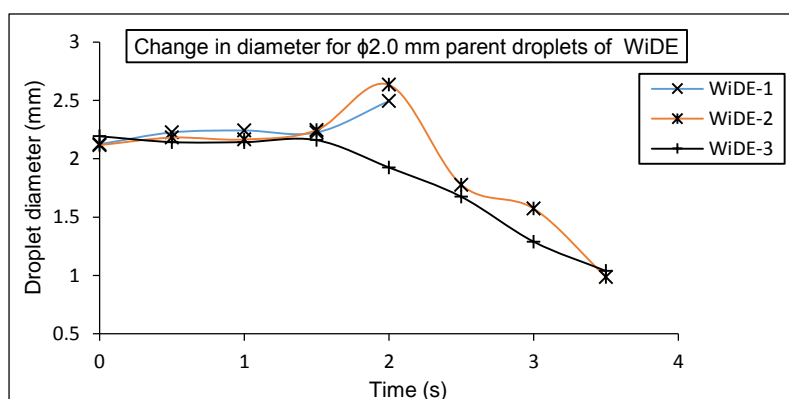


**Figure 10.** Change in diameter of  $\phi 2.0$  mm WiDE droplets at every 0.5s interval

Figures 9 and 10 depict the changes in the diameter of the parent droplet at half second time interval. For both cases there were no significant changes in the droplet diameter up to 1.5 s, due to the fact that the droplet might not had enough heating energy. As the time increases the droplet diameter started increasing due to vapour expansion inside the droplet. As the pressure built up in the droplet and reached a particular point it was released in the form of puffing. Puffing is the ejection of the inner content of the emulsified droplet without the complete shattering of the parent droplet. At the end of every puffing (resulting in ejection of larger child droplets) the diameter of the parent droplet dropped and underwent further vapour expansion and its diameter increased as

shown in the graph. The time taken for initial puffing and the puffing frequency of  $\phi 2.6$  mm and  $\phi 2.0$  mm WiDE droplets are shown in Figure 11.

The time taken for initial puffing and the puffing frequency of  $\phi 2.6$  mm and  $\phi 2.0$  mm WiDE droplets are shown in Figure 11. The time taken for initial puffing was found to increase with increasing water content in the case of  $\phi 2.6$  mm droplet diameter whereas no such trend was observed in the case of  $\phi 2.0$  mm diameter droplets. However, it is clear from the Figure 11 that the time taken for the initial puffing was considerably less in the case of smaller droplet of WiDE.

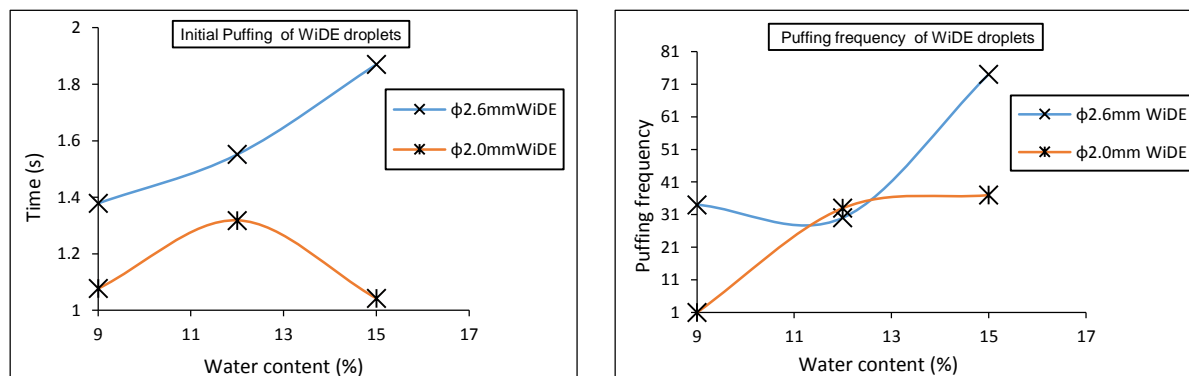


**Figure 11.** Time taken for initial puffing and the puffing frequency of  $\phi 2.6$  mm and  $\phi 2.0$  mm WiDE droplets

As far as the puffing frequency is concerned, it was comparatively higher for the  $\phi 2.6$  mm droplet than the  $\phi 2.0$  mm. Notably, WiDE-3 with 15% water content exhibited maximum puffing frequency irrespective of the droplet diameters. It was found that the parent droplet size played an important role in the puffing frequency with the larger parent droplets producing high puffing frequencies.

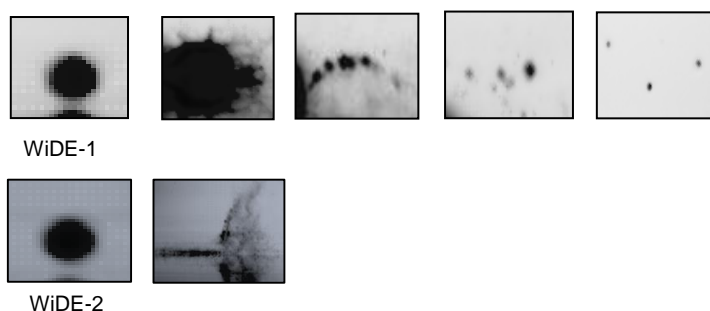
As highlighted in the Figure 12, the child droplets ejected from the parent droplet during puffing was observed to undergo further puffing. The ejected child droplet was about  $\phi 0.568$  mm. The child droplet was ejected at 1.590s from the parent droplet and the puffing time for the child droplet was at 1.5921s.



**Figure 12.** Puffing of a child droplet of  $\phi 0.5681$  mm ejected from of parent droplet of  $\phi 2.6$  mm

### Microexplosion and puffing behaviour of smaller WiDE droplets

The microexplosion evolutions of the smaller droplets of  $\phi 0.2$  mm to  $\phi 0.3$  mm are discussed in this section. These droplets were generated by dropping a larger droplet from a height onto the hot plate which resulted in the production of smaller droplets. Since it was not possible to control the size or the movement of the droplets generated this way, only selected droplets which underwent microexplosion were considered for analysis excluding bouncing droplets. These images were captured at 10000 fps. The microexplosion behaviour of smaller droplets of WiDE-1, 2 and 3 are shown in Figure 13.



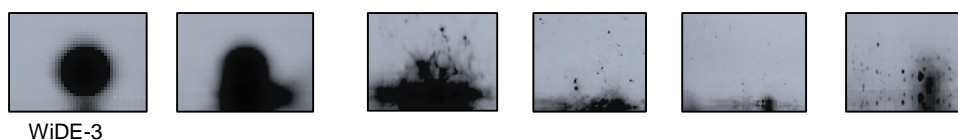


**Figure 13.** Microexplosion of smaller parent WiDE droplets and secondary droplets

**Table 4.** Waiting time of smaller droplets of WiDE

Sample ID	Droplet diameter (mm)	Microexplosion time (s)	Average diameter of secondary droplets after microexplosion (mm)
WiDE-1	0.17	0.196	0.053
WiDE-2	0.23	0.152	0.031
WiDE-3	0.30	0.233	0.030

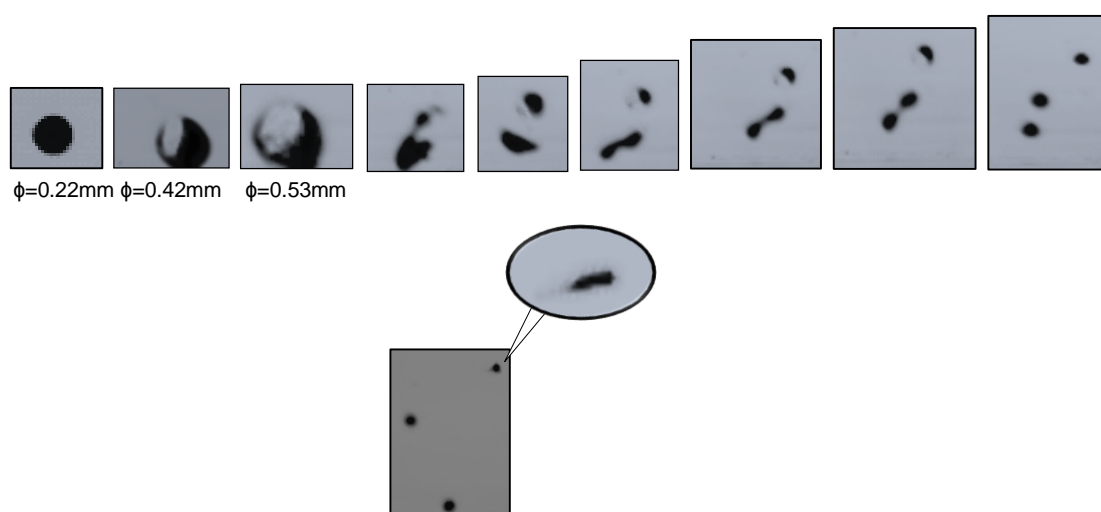


**Figure 14.** Puffing sequence of a parent droplet of diameter  $\phi 0.224\text{mm}$ , resulting in ejection of child droplets

The waiting times of the parent droplets and the size of the secondary droplets after microexplosion are shown in Table 4. The secondary droplets created after microexplosion of parent droplets were between 1/3 and 1/10 of the size of the parent droplets. Figure 14 shows the instantaneous images of a puffing sequence of WiDE-2, which was observed with the smaller parent droplet of  $\phi 0.2\text{ mm}$  and resulted in child droplets of  $\phi 0.135\text{ mm}$  and  $\phi 0.138\text{ mm}$ . The duration of puffing was  $0.002\text{ s}$ . As shown in Figure 14, the diameter of the parent droplet increased due to vapour expansion and resulted in the puffing of child droplets. The ejected child droplets were observed to undergo further puffing processes as shown.

## Conclusions

Water in pure diesel emulsion (WiDE) with different parent droplet sizes were visualized for the microexplosion evolution and the outcomes of the observation are summarised as follows;

- Coalescence was the dominant factor in inducing the microexplosion phenomenon in the case of large droplets.
- Puffing frequency of the WiDE droplets was a function of the parent droplet size.
- The child droplets ejected during puffing of parent droplets underwent further puffing processes.
- Unlike the large diameter droplets, the small sized ( $\phi 0.2\text{ mm}$ ) WiDE droplets developed microexplosion irrespective of their water content.
- The size of the child droplets after microexplosion was almost less than 1/10 of the size of the parent droplet for large droplets ( $\phi 2.6$  and  $\phi 2.0\text{ mm}$ ) and between 1/3 and 1/10 of the size of the smaller parent droplet.



## Acknowledgements

The authors wish to thank the Universiti Teknologi PETRONAS for the financial and facility support for the study. The authors express their gratitude to Firmansyah and Ezrann Zharif for their technical assistance in conducting the experiments.

## References

- [1] Watanabe, H., Suzuki, Y., Harada, T., Matsushita, Y., Aoki, H., and Miura, T., 2010, "An experimental investigation of the breakup characteristics of secondary atomization of emulsified fuel droplet," *Energy*, 35(2), pp. 806-813.
- [2] Calabria, R., Chiariello, F., and Massoli, P., 2007, "Combustion fundamentals of pyrolysis oil based fuels," *Experimental Thermal and Fluid Science*, 31(5), pp. 413-420.
- [3] Tsue, M., Kadota, T., Segawa, D., and Yamasaki, H., 1996, "Statistical analysis of onset of microexplosion for an emulsion droplet," *Proc. Symposium (International) on Combustion*, Elsevier, pp. 1629-1635.
- [4] Watanabe, H., Harada, T., Matsushita, Y., Aoki, H., and Miura, T., 2009, "The characteristics of puffing of the carbonated emulsified fuel," *International Journal of Heat and Mass Transfer*, 52(15), pp. 3676-3684.
- [5] Califano, V., Calabria, R., and Massoli, P., 2014, "Experimental evaluation of the effect of emulsion stability on micro-explosion phenomena for water-in-oil emulsions," *Fuel*, 117, pp. 87-94.
- [6] Avulapati, M. M., Ganippa, L. C., Xia, J., and Megaritis, A., 2016, "Puffing and micro-explosion of diesel–biodiesel–ethanol blends," *Fuel*, 166, pp. 59-66.
- [7] Khan, M. Y., Abdul Karim, Z. A., Aziz, A. R. A., and Tan, I. M., 2014, "Experimental Investigation of Microexplosion Occurrence in Water in Diesel Emulsion Droplets during the Leidenfrost Effect," *Energy & Fuels*, 28(11), pp. 7079-7084.
- [8] Yahaya Khan, M., Abdul Karim, Z., Aziz, A. R. A., and Tan, I. M., 2016, "Experimental Study on Influence of Surfactant Dosage on Micro Explosion Occurrence in Water in Diesel Emulsion," *Applied Mechanics and Materials*, 819, pp. 287-291.
- [9] Ocampo-Barrera, R., Villasenor, R., and Diego-Marin, A., 2001, "An experimental study of the effect of water content on combustion of heavy fuel oil/water emulsion droplets," *Combustion and flame*, 126(4), pp. 1845-1855.
- [10] Tanaka, H., Kadota, T., Segawa, D., Nakaya, S., and Yamasaki, H., 2006, "Effect of ambient pressure on micro-explosion of an emulsion droplet evaporating on a hot surface," *JSME International Journal Series B*, 49(4), pp. 1345-1350.
- [11] Morozumi, Y., and Saito, Y., 2010, "Effect of physical properties on microexplosion occurrence in water-in-oil emulsion droplets," *Energy & Fuels*, 24(3), pp. 1854-1859.
- [12] Suzuki, Y., Harada, T., Watanabe, H., Shoji, M., Matsushita, Y., Aoki, H., and Miura, T., 2011, "Visualization of aggregation process of dispersed water droplets and the effect of aggregation on secondary atomization of emulsified fuel droplets," *Proceedings of the Combustion Institute*, 33(2), pp. 2063-2070.
- [13] Tarlet, D., Mura, E., Josset, C., Bellettre, J., Allouis, C., and Massoli, P., 2014, "Distribution of thermal energy of child-droplets issued from an optimal micro-explosion," *International Journal of Heat and Mass Transfer*, 77, pp. 1043-1054.
- [14] Mura, E., Calabria, R., Califano, V., Massoli, P., and Bellettre, J., 2014, "Emulsion droplet micro-explosion: Analysis of two experimental approaches," *Experimental Thermal and Fluid Science*, 56, pp. 69-74.
- [15] Abdul Karim, Z. A., Khan, M. Y., A. Aziz, A. R., and Tan, I. M., 2014, "Characterization of Water in Diesel Emulsion," *MATEC Web of Conferences*, 13, p. 02006.
- [16] Wasan, D., Nikolov, A., and Aimetti, F., 2004, "Texture and stability of emulsions and suspensions: role of oscillatory structural forces," *Advances in colloid and interface science*, 108, pp. 187-195.